Pergamon

Tetrahedron, Vol. 53, No. 1, pp. 225-236, 1997

0040-4020/97 $17.00 + 0.00

PII: S0040-4020(96)00965-9

Theoretical Study of the Reaction of Silylketenes with Acyl Isocyanates

Takatoshi Matsumoto,* Kiyo Takaoka, Toyohiko Aoyama, and Takayuki Shioiri*

Department of Synthetic Organic Chemistry, Faculty of Pharmaceutical Sciences, Nagoya City University, Tanabe-dori, Mizuho-ku, Nagoya 467, Japan

Abstract : The reaction of silylketenes with acyl isocyanates followed by the hetero Diels-Alder reaction with acetylene derivatives has been investigated at the AM1 semi-empirical level. A series of these reaction pathways has been revealed in detail.

Silylketenes have been known as interesting reagents having high reactivity like ketenes but are more stable, can withstand long-term storage and are easier to handle. Recent publications from our laboratories have disclosed that [4+2] cycloaddition reaction of silylketenes with electron-rich 1,3-dienes and *o*-quinodimethanes gives 2-pyranones and isochromenes, respectively,[1] and that enamines easily undergo a novel type cycloaddition reaction with an excess of silylketenes to give resorcinol derivatives.[2] Furthermore, we have revealed that trimethylsilylketene (**1**) reacts with acyl isocyanates (**2**) to give the 1,3-oxazin-6-ones (**3**) and the labile **3** easily reacts with some acetylenes (**4**) to produce 2-pyridones (**6**) via the 2-siloxypyridine derivatives (**5**).[3] Because this reaction sequence is worthy of note from the viewpoint of the site selectivity and high chemical yields, we have theoretically investigated these reactions at the AM1 semi-empirical level, using benzoyl isocyanate (**2**, R^1=Ph) and methyl propiolate (**4**, R^2=H).

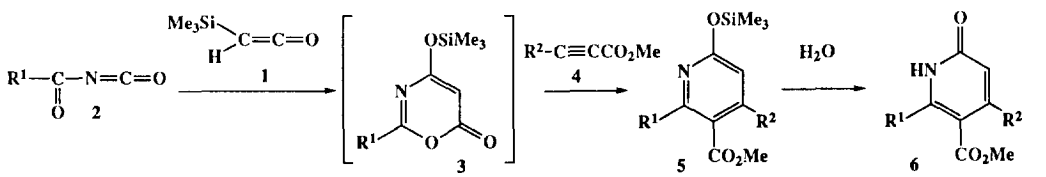

Scheme 1. The reaction of silylketenes with acyl isocyanates followed by the hetero Diels-Alder reaction with acetylene derivatives.

AM1 semi-empirical molecular orbital calculations were performed by MOPAC 93[4] on a Titan 2-800 and an AlphaServer 2100 5/250 workstation. Input coordinates were built with the CSC Chem 3D plus Ver. 3.1 on a Power Macintosh 8100/80 personal computer. The geometry was optimized using the PRECISE option in order to decrease the gradient norm. The respective transition states for the respective reaction steps were located using the TS method[5a] and the SADDLE routine[5b] implemented in MOPAC 93 and characterized by establishing that the force constant matrix had only one negative

frequency. To verify that calculated transition states connect reactants and products, AM1 level intrinsic reaction coordinate (IRC) calculations[5c] were carried out with respect to each transition state.

First, we examined some model compounds (**2**, **7**-**10**) in order to check the structural properties and the relationship between the positions of functional groups and thermodynamic stability (Figure 1). For benzoyl isocyanate (**2**), it was most stable when all atoms existed in a plane. The reason was that the continuous and long π-conjugated system contributed to the thermodynamic and structural stabilities. As for the model compound (**7**), it was most stable when the position of the hydroxyl function was level with the ring and directed forward the nitrogen atom side. Regarding the model compound (**8**), it was also most stable when the position of the hydroxyl function was level with the ring and directed forward the oxygen atom side. The comparison between **7** and **8** made it clear that **7** was more stable than **8** from the view of relative energy and that the continuity of the π-conjugated system contributed to the thermodynamic and structural stabilities. Compound **9** was most stable when the two rings were at the same levels. When the trimethylsilyl function was directed toward the nitrogen atom, **10** was most stable. In the case of the opposite direction, **10** was metastable.

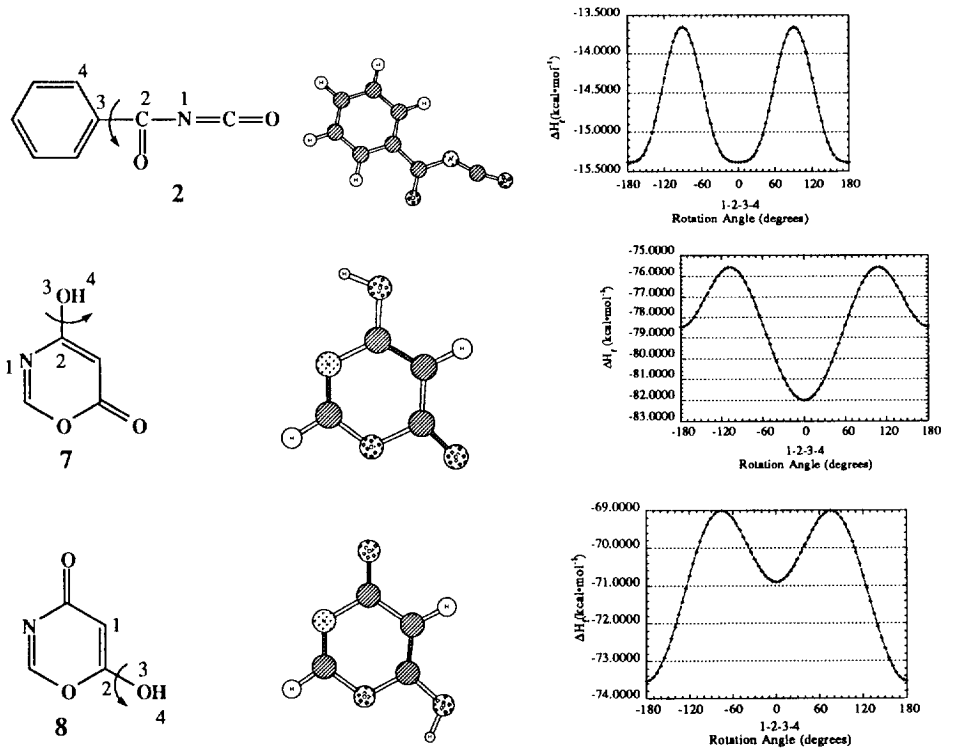

Figure 1.1. The global minimum structures and the rotational energy charts for the model compounds

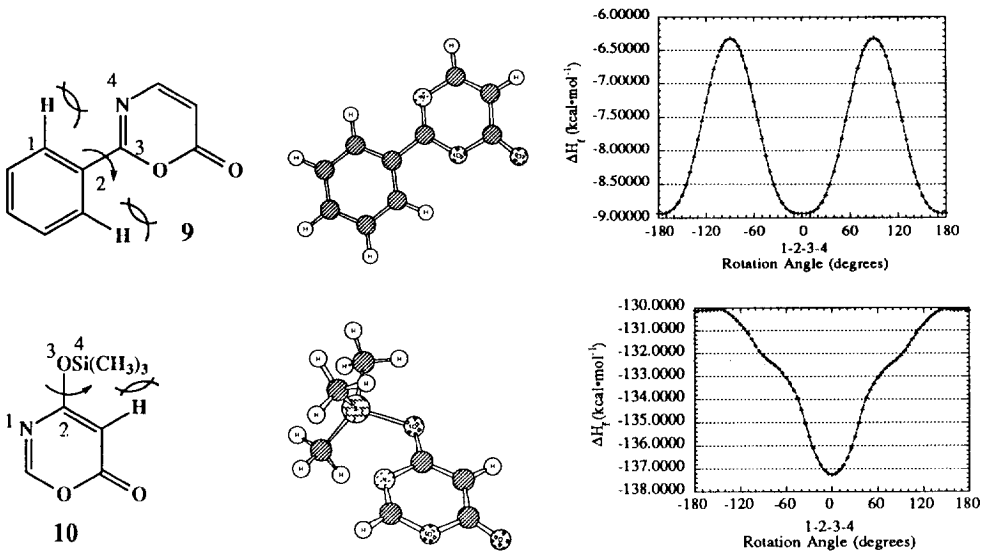

Figure 1.2. The global minimum structures and the rotational energy charts for the model compounds

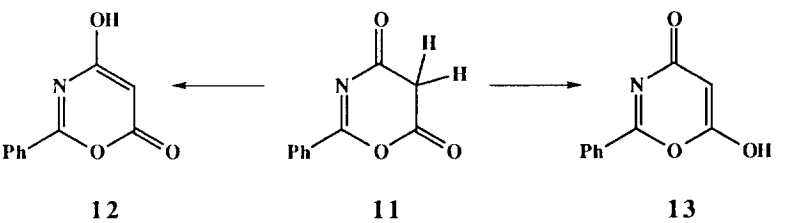

Scheme 2. The simple and similar keto-enol tautomerism for 2-phenyl-1,3-oxazine-4,6-dione (**11**)

Zakhs et al. studied the tautomerism for 2-phenyl-1,3-oxazine-4,6-dione (**11**) and described that **12** was energetically more favored than **13** based on quantum chemical calculations.[6] However, their explanation and calculations were insufficient and ambiguous. In order to obtain the properties of tautomerism, transition states, and thermodynamic stability, we studied the simple and similar keto-enol tautomerism for **11** again (Scheme 2). We surveyed the stable structures in the rotational isomers **12** and **13** in regard to the geometrical properties using some model compounds in Figure 2. The structure **12a** was found to be the most stable state when the position of the hydroxyl function was level with the ring and the direction toward the nitrogen atom side. The structure **12b** was also found to be the metastable state, while the structure **13a** was the most stable one when the position of the hydroxyl function was level with the ring and the direction toward the oxygen atom side. The structure **13b** was the metastable one, too. This reexamination of thermodynamic stability made it apparent that the structure **12** in which the continuity of the π-conjugated system was maximum was the most stable relative to the structure **13**.

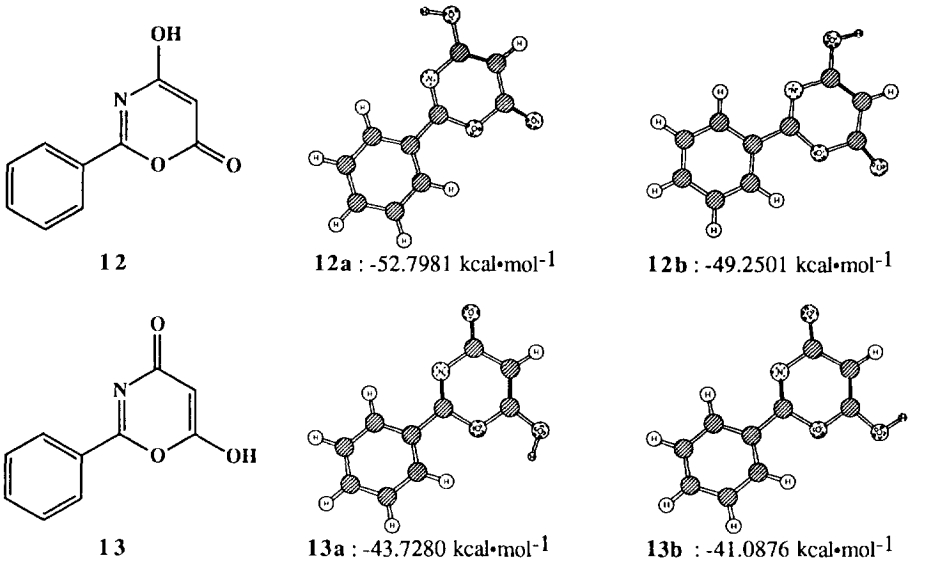

Figure 2. The minimum energy structures of the tautomeric isomers for **11**

Next we calculated the energy barriers and transition states when the tautomeric isomer **11** shifted to **12** or **13**.[7] The transition state structure **14** was found in the middle of the pathway from **11** to **12**, while **15** was also found to be in the middle of the pathway from **11** to **13** (Figure 3 and Table 1). The obtained transition state structures had only one negative frequency, respectively, and the calculated transition states connected the reactants and products with the IRC calculations. The obtained energy relation is shown in Figure 4. Because the activated energy barrier of this keto-enol tautomerism for **14** was 11.2882 kcal•mol^{-1} less than that of **15**, this result pointed out that **11** shifted toward **12** via the transition state **14**.

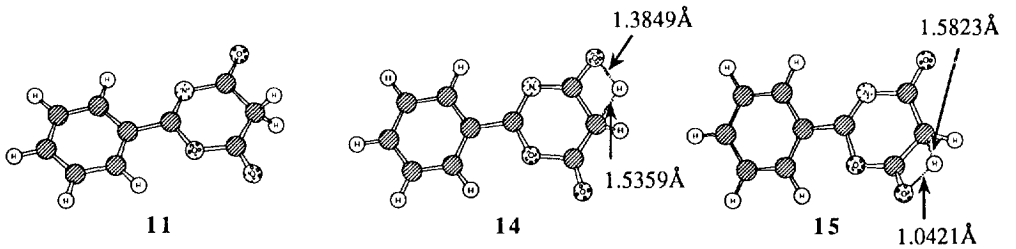

Figure 3. The structures of **11** and transition states **14** and **15**

Table 1. Data for **11** and transition states **14** and **15**

	ΔH_f /kcal•mol^{-1}	Frequency /cm^{-1}	Length of C - H /Å	Length of O - H /Å
11	-52.8556	———	1.1259	———
14	18.1318	2429.4*i*	1.5359	1.3849
15	29.4200	2515.4*i*	1.5823	1.4021

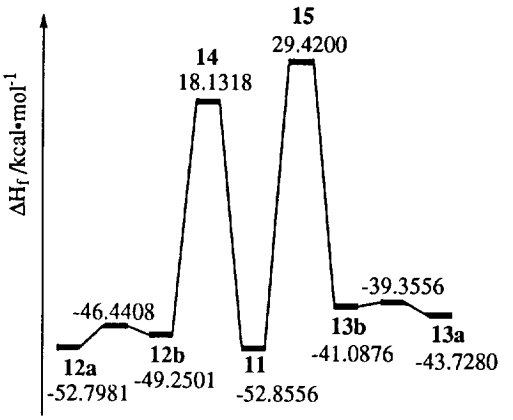

Figure 4. The calculated energetic relation to the respective structures

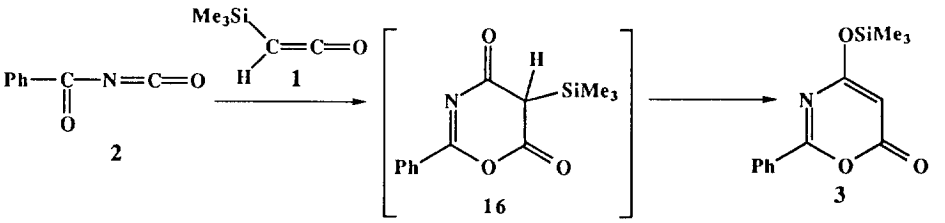

Scheme 3. The reaction of trimethylsilylketene (**1**) with phenyl isocyanate (**2**)

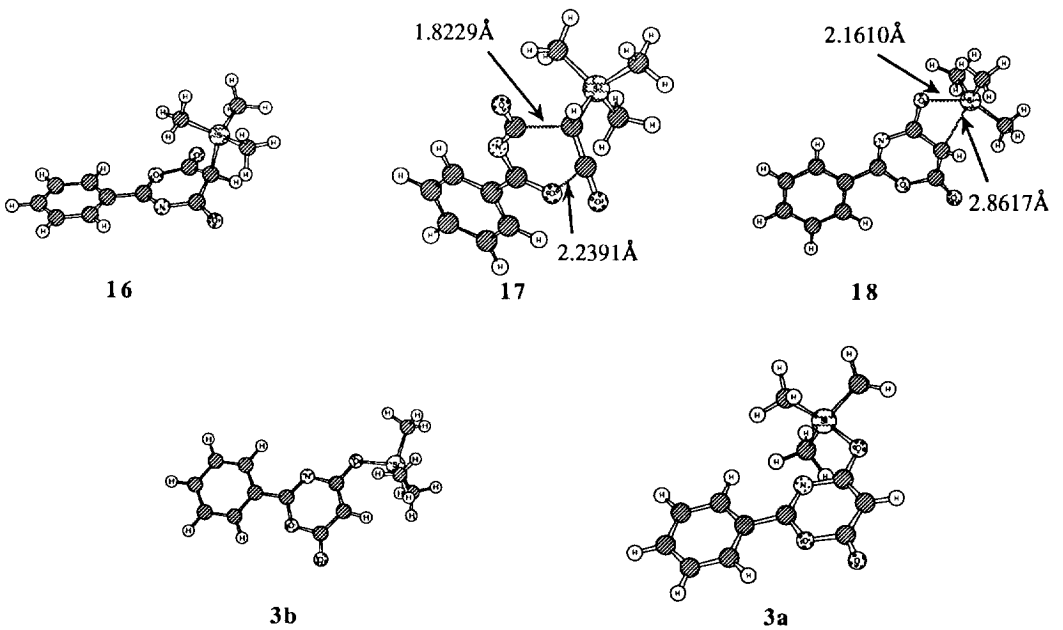

Figure 5. The structures of reaction intermediate **16**, transition states **17** and **18**, and rotational isomers **3**

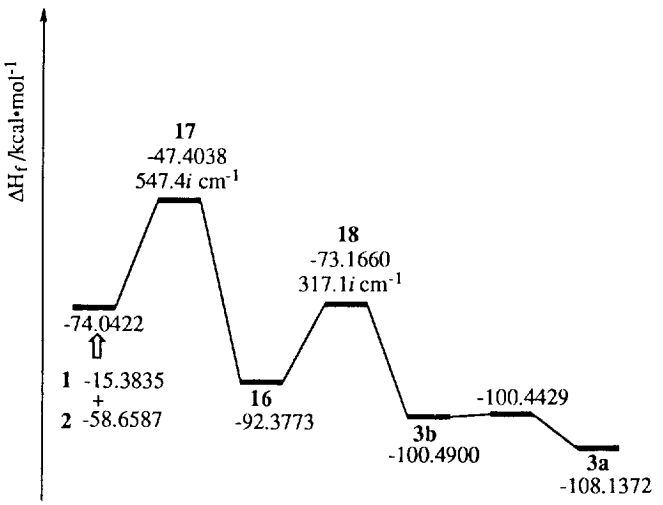

Figure 6. The calculated energetic relation to the respective structures

The simple and similar keto-enol tautomerism for **11** was clarified in detail, therefore, we investigated the reaction pathway including the transition states when **1** reacts with **2** (Scheme 3).[8-10] The transition state **17** involved cyclization to form a 1,3-oxazine ring when the first step of this reaction occurred. When the second step of the reaction occurred, the transition state **18** involved the shift of the trimethylsilyl function (Figure 5). No reaction intermediates except **16** could be found. The calculated transition states connected the reactants and the products with the IRC calculations, and the results of the IRC calculation then made it clear that the first step of the reaction proceeded by a concerted cyclization process. The obtained energy relation is shown in Figure 6.

We also investigated another tautomeric isomer **19** in order to determine the direction in which the trimethylsilyl function shifted and to compare the relative energy of the transition states when the trimethylsilyl function shifted (Scheme 4). From the influence based on the case of the simple and similar tautomerism of **11**, we assumed that this function shift would need a high activated energy. The transition state **20** was found in the middle of the pathway from **16** to **19**. The obtained structure and energy relation of the pathway are shown in Figures 7 and 8, respectively. In comparison with the energy of the transition states, **20** was 7.4822 kcal•mol^{-1} higher than **18**. We supposed that the direction in which the trimethylsilyl function shifted was not from **16** to **19** but from **16** to **3** because of the relatively large energy barrier.

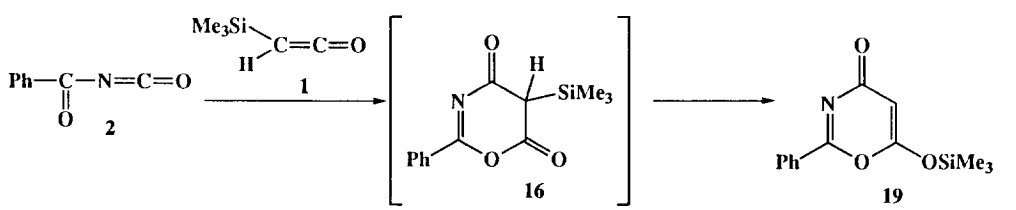

Scheme 4. Another reaction pathway when **1** reacts with **2**

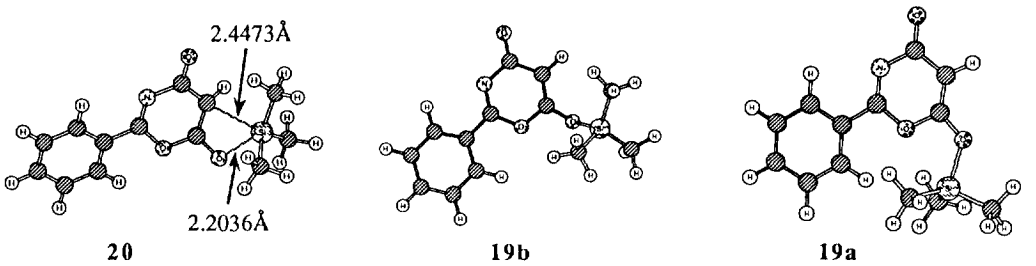

Figure 7. The calculated structure of transition state **20** and rotational isomers **19**

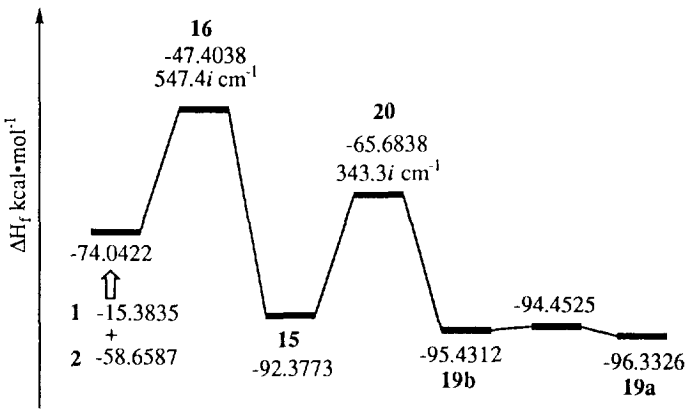

Figure 8. The calculated energetic relation to the respective structures

Path A

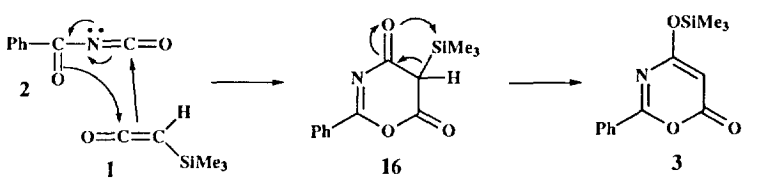

Path B

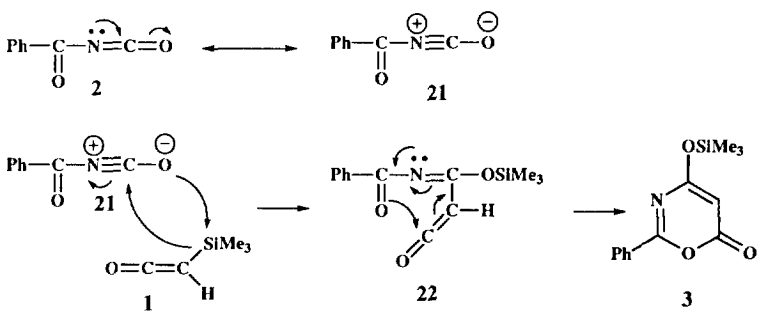

Scheme 5. The possible two reaction pathways by the reaction mechanism based on the organic electronic theory

There were two possible reaction pathways from the viewpoint of the reaction mechanism based on the organic electronic theory (Scheme 5). One was the pathway proceeding by a concerted cyclization process and then the shift of the trimethylsilyl function (Path A). The other was the pathway occurring by the stepwise cyclization process (Path B). Regarding the latter pathway, we tried all methods in order to verify whether this route existed. The former pathway was sometimes easily found when we searched for the latter, but we could not find out the latter pathway. From our calculation results, we supposed that this reaction proceeded by the former pathway.

Furthermore, we investigated the reaction of the oxazine derivative (**3**) with methyl propiolate (**4**) (Scheme 6). Before the inquiry about the reaction pathway and transition states, the molecular orbitals used and the distribution of the net atomic charges for **3** and **4** were studied in detail (Tables 2-4). The states of the orbitals used based on the coefficients of the eigenvectors for the respective compounds are shown in Figure 9. From the obtained results, we regarded this reaction as a sort of hetero Diels-Alder reaction and a thermodynamically allowed type. The reaction proceeded with a LUMO of **4** and a HOMO of **3**. In order to fit the phases of the respective molecular orbitals and to achieve the maximum for overlap of molecular orbitals, the site selectivity arose to the products (Figure 10).

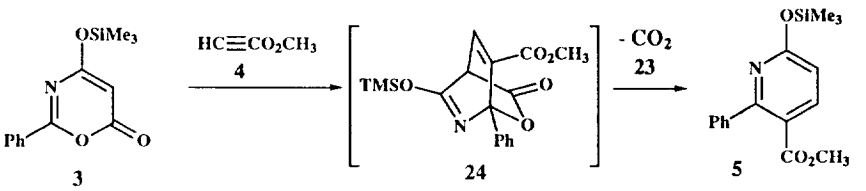

Scheme 6. The reaction of the oxazine derivative (**3**) with methyl propiolate (**4**)

Table 2. Data of the energy of the used orbitals

Material	HOMO	LUMO
4	-11.534	0.023
3	-9.339	-1.048

Table 3. Data for the minimum energy structure, the distribution of atomic net charges and the coefficients of eigenvectors for **4**

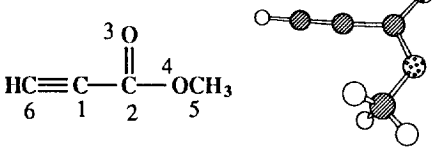

Atom Coordinate Number

Atom No.	Eigenvectors of the Pz direction	Atom No.	Atomic Net Charges
1	-0.4192	1	-0.2308
2	-0.5154	2	0.4140
3	0.4169	3	-0.2747
4	0.1816	4	-0.2423
5	0.0340	5	-0.0733
6	0.5891	6	-0.0935

Table 4. Data for the minimum energy structure, the distribution of atomic net charges and the coefficients of eigenvectors for **3**

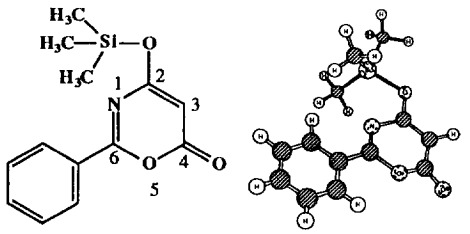

Atom No.	Eigenvectors of the Pz direction	Atom No.	Atomic Net Charges
1	-0.2697	1	-0.3302
2	0.2793	2	0.2450
3	0.6746	3	-0.3652
4	0.0687	4	0.3565
5	0.0657	5	-0.2428
6	-0.2147	6	0.2556

Atom Coordinate Number

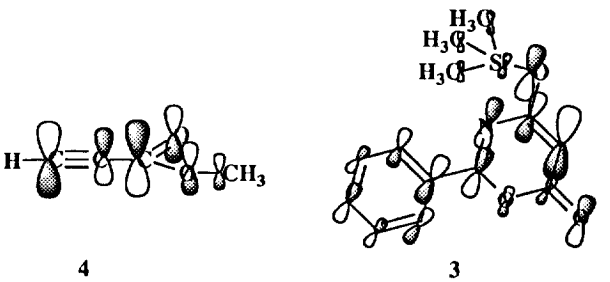

4 3

Figure 9. The states of the respective orbitals used

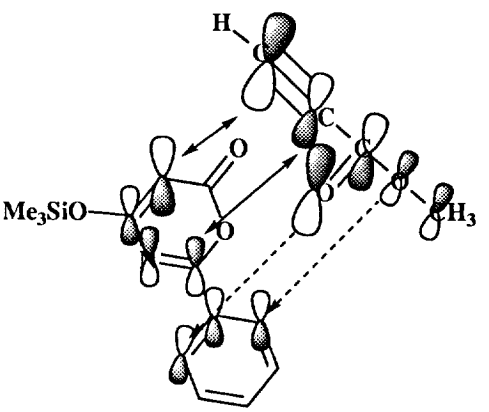

Figure 10. The orbital interaction for the reaction of the oxazine derivative (**3**) with methyl propiolate (**4**)

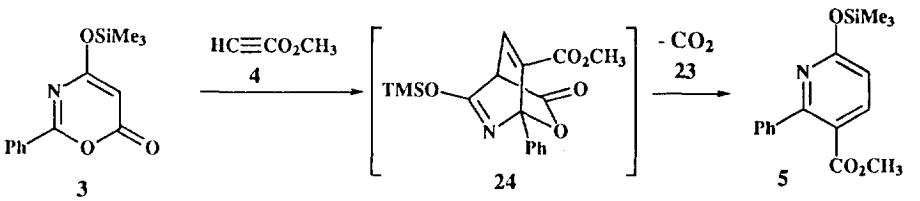

Scheme 7. The reaction of the oxazine derivative (**3**) with methyl propiolate (**4**)

Finally, we explored the reaction pathway including the transition states when **3** reacted with **4** (Scheme 7).[11] When the first step of this reaction advanced, the transition state **25** was the combination of two compounds. The transition state **26** involved the elimination of carbon dioxide (**23**) when second step of the reaction proceeded (Figure 11). No reaction intermediates except for **24** could be found. The calculated transition states connected the reactants and the products with the IRC calculations, and the results of the IRC calculation made it clear that the reaction proceeded by a concerted process. The obtained energy relation is shown in Figure 12.

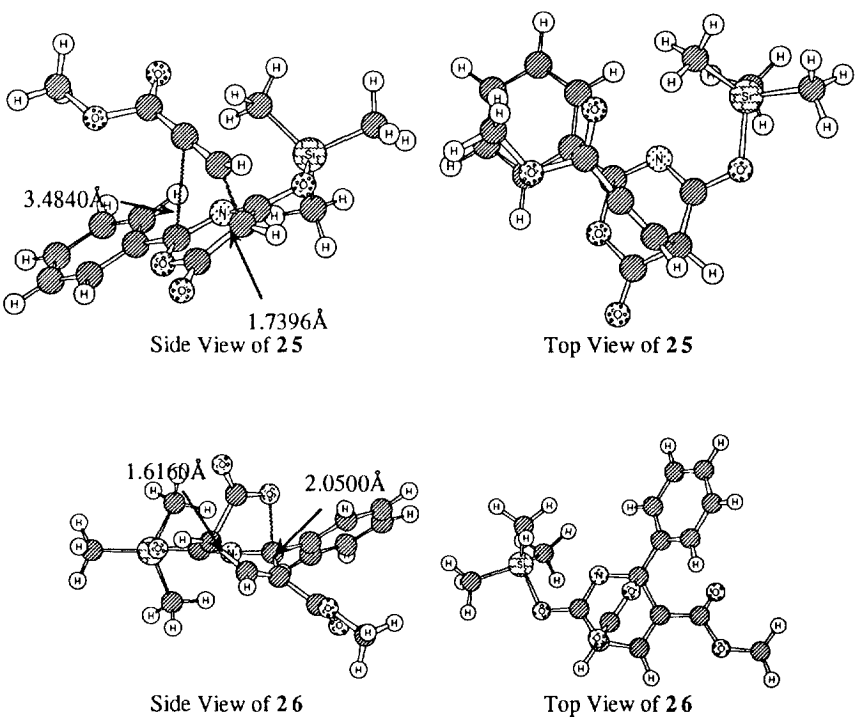

Figure 11 The calculated structure of the transition states **25** and **26**

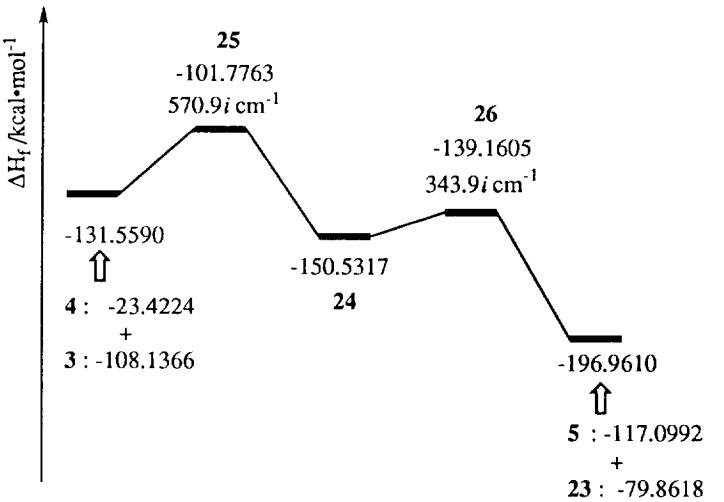

Figure 12. The calculated energetic relation to the respective structures

In conclusion, the results at the AM1 semi-empirical level have revealed a series of reaction pathways for the reaction of trimethylsilylketene (**1**) with benzoyl isocyanate (**2**) followed by the hetero Diels-Alder reaction with methyl propiolate (**4**), which have clarified the properties for regioselectivity and transition states.

References and Notes

1. Ito, T.; Aoyama, T.; Shioiri, T. *Tetrahedron Lett.*, **1993**, *34*, 6583.
2. Takaoka, K.; Aoyama, T.; Shioiri, T. *Synlett*, **1994**, 1005.
3. (a) Takaoka, K.; Aoyama, T.; Shioiri, T. *Tetrahedron Lett.*, **1996**, *37*, 4973. (b) Takaoka, K.; Aoyama, T.; Shioiri, T. *Tetrahedron Lett.*, **1996**, *37*, 4977
4. MOPAC 93.00, Stewart, J.J.P., Fujitsu Ltd., Tokyo, Japan, 1993. Available from Quantum Chemistry Program Exchange, University of Indiana, Bloomington, IN.
5. (a) Baker, J.. *J. Comput. Chem.*, **1989**, *10*, 210., (b) Dewar, M.J.S.; Healy, E.F.; Stewart, J.J.P. *J. Chem. Soc. Faraday Trans. II*, **1984**, *3*, 227. (c) Dieter, K.M.; Stewart, J.J.P. *J. Mol. Struct. (Theochem)*, **1988**, *163*, 143.
6. (a) Zakhs, V.É; Yakovlev, I.P.; Smorygo, N.A.; Gindin, V.A.; Ivin, B.A. *Khim. Geterotsikl. Soedin.*, **1987**, 3, 386. (b)Zakhs, V.É.; Yakovlev, I.P.; Tret'yakov, A.A.; Gindin, V.A.; Prep'yalov, A.V.; Ivin, B.A. *Zh. Org Khim.*, **1991**, *27*, 864. (c) Yakovlev, I.P.; Zakhs, V,É.; Prep'yalov, A.V.; Ivin, B.A. *Zh. Org Khim.*, **1993**, *63*, 2082.
7. (a) Yliniemelä, A.; Konschin, H.; Neagu, C.; Pajunen, A.; Hase, T.; Brunow, G.; Teleman, O. *J. Am. Chem. Soc.*, **1995**, *117*, 5120. (b) Metzanos, G.E.; Alexandrou, N.E.; Tsoleridis C.A.; Mitkidou, S.; Stephanidou-Stephanatou, J. *Heterocycles*, **1994**, *37*, 967. (c) Tomioka, H.; Nitta, M. *Heterocycles*, **1994**, *38*, 629. (d) Matsuoka T.; Harano K. *Tetrahedron*, **1995**, *51*, 6451.

8. Domingo, L.R.; Jones, R.A.; Picher, M.T.; Sepúlveda-Arques, J. *Tetrahedron*, **1995**, *51*, 8739.
9. Valentí, E.; Pericás, M.A.; Moyano, A. *J. Org. Chem.*, **1990**, *55*, 3582.
10. (a) Martin, J.C.; Burpitt, R.D.; Gott, P.G.; Harris, H.; Meen, R.H. *J. Org. Chem.*, **1971**, *36*, 2205. (b) Martin, J.C.; Brannock, K.C.; Burpitt, R.D.; Gott, P.G.; Hoyle, V.A.Jr. *J. Org. Chem.*, **1971**, *36*, 2211.(c) Chutwood, J.L.; Gott, P.G.; Krutak, J.J.Jr.; Martin, J.C. *J. Org. Chem.*, **1971**, *36*, 2216. (d) Burpitt, R.D.; Brannock, K.C.; Nations, R.D.; Martin, J.C. *J. Org. Chem.*, **1971**, *36*, 2222. (e) Chitwood, J.L.; Gott, P.G.; Martin, J.C. *J. Org. Chem.*, **1971**, *36*, 2228., (f) Seikaly, H.R.; Tidwell, T.T. *Tetrahedron*, **1986**, *42*, 2587.
11. (a) Dewar, M.J.S.; Olivella, S.; Stewart, J.J.P. *J. Am. Chem. Soc.*, **1986**, *108*, 5771. (b) Bernardi, F.; Bottoni, A.; Robb, M.A.; Field, M.J.; Hillier, I.H.; Guest, M.F. *J. Chem. Soc. Chem. Commun.*, **1985**, 1051. (c) Dewar, M.J.S.; Merz, K.M.Jr. *J. Am. Chem. Soc.*, **1986**, *108*, 5142.(d) Houk, K.H.; Gonzál ez, J.; Li, Y. *Acc. Chem. Res.*, **1995**, *28*, 81. (e) Somekawa, K.; Shimo, T.; Suishu, T. *Bull. Chem. Soc. Jpn.*, **1992**, *65*, 354.

(*Received in UK* 9 *September* 1996; *revised* 14 *October* 1996; *accepted* 17 *October* 1996)